

## A novel pore size classification method of coals: Investigation based on NMR relaxation

Sijian Zheng<sup>a,b,c</sup>, Yanbin Yao<sup>a,b,\*</sup>, Derek Elsworth<sup>d</sup>, Bo Wang<sup>e</sup>, Yong Liu<sup>a,b</sup>

<sup>a</sup> School of Energy Resource, China University of Geosciences, Beijing, 100083, China

<sup>b</sup> Coal Reservoir Laboratory of National Engineering Research Center of CBM Development & Utilization, China University of Geosciences, Beijing, 100083, China

<sup>c</sup> Beijing Key Laboratory of Unconventional Natural Gas Geological Evaluation and Development Engineering, China University of Geosciences, Beijing, 100083, China

<sup>d</sup> Department of Energy and Mineral Engineering, Pennsylvania State University, University Park, PA, 16802, USA

<sup>e</sup> Information Institute, Ministry of Emergency Management of PR China, Beijing, 100029, China

### ARTICLE INFO

#### Keywords:

NMR  
Pore size distribution  
Pore classification  
Dual  $T_2$  cutoffs  
Coalbed methane

### ABSTRACT

Nuclear magnetic resonance (NMR) serves as a nondestructive and relative new technique that has been widely used in characterizing reservoir fluids and pore size distribution (PSD) of coals. Conventionally, pore fluids in coals are classified into movable fluid and irreducible fluid based on a single NMR  $T_2$  cutoff value ( $T_{2C}$ ). However, the single NMR  $T_2$  cutoffs model has some apparent defects in pore fluid/size classification, and few researches have reported the limitation of the single  $T_2$  cutoffs model. In contrast, the dual  $T_2$  cutoffs model may provide an accurate quantified model to classify different pore fluid types in coals. In this study, fifteen coal samples with different ranks were conducted in systematic NMR and centrifugal experiments to investigate the characteristics of pore fluid typing and PSD. Results show that when tried applying the single NMR  $T_2$  cutoffs model to classify the pore fluid typing, there are still some movable fluids when  $T_2 < T_{2C}$ . At the same time, when  $T_2 > T_{2C}$ , there is remaining some irreducible fluid in pores after high pressure centrifugal experiments. These results indicated the limited application of single NMR  $T_2$  cutoffs model in pore fluid classification. By introducing a novel pore fluid classification method (i.e. the dual  $T_2$  cutoffs model), a typical  $T_2$  spectrum under fully-saturated condition, the absolute irreducible fluid  $T_2$  cutoffs ( $T_{2C1}$ ) and absolute movable fluid  $T_2$  cutoff ( $T_{2C2}$ ) can re-divide the pore fluid typing of coal into three types: absolute irreducible fluid ( $T_2 < T_{2C1}$ ), partial movable fluid ( $T_{2C1} < T_2 < T_{2C2}$ ), and absolute movable fluid ( $T_2 > T_{2C2}$ ). The results show that the  $T_{2C1}$  is in the range of 0.10–0.32 ms, while the  $T_{2C2}$  has a wider range from 36.12 ms to 89.07 ms. Finally, a conceptual model were proposed to clarify a full-scale PSD classification that includes the absolute irreducible fluid pores, partial movable fluid pores and absolute movable fluid pores. The model established in this study, can also be applicable for other rock types (e.g., sandstones, carbonates and shales).

### 1. Introduction

High-efficiency coalbed methane (CBM) development is of importance in some counties (e.g. Australia, Canada and China) since it can better decrease greenhouse gas emissions, ensure coal production safety, and provide clean energy (Karacan et al., 2011; Moore, 2012). The rapid development of CBM industry has drawn much attention to coal petrophysical property investigations, like pore fluid characterization, pore size distribution (PSD), wettability and permeability (Weniger et al., 2012; Zhao et al., 2017; Du et al., 2019; Yao et al., 2019). The PSD is one of the important parameters to comprehensively analyze the flow and storage capacities of gas and water in coal, and the prediction of CBM

production (Close, 1993; Clarkson and Bustin, 1999). Thus, an accurate quantitative characterization of the PSD in coals is key for CBM production.

Currently, various updated methods have been used to characterize coal PSD, such as imaging analysis methods, fluid intrusion methods and nonintrusive fluid methods. Image analysis methods include high resolution scanning electron microscope (SEM), atomic force microscopy (AFM) and transmission electron microscopy (TEM). Fluid intrusion methods, including mercury intrusion porosity (MIP) and gas adsorption ( $N_2$  and  $CO_2$ ). Nonintrusive fluid methods, including X-ray computerized tomography (X-CT) and small-angle neutron scattering (SANS). However, some of these methods have certain limitations in

\* Corresponding author. School of Energy Resource, China University of Geosciences, Beijing, 100083, China.

E-mail addresses: [yyb@cugb.edu.cn](mailto:yyb@cugb.edu.cn), [yaoyanbin@126.com](mailto:yaoyanbin@126.com) (Y. Yao).

<https://doi.org/10.1016/j.jngse.2020.103466>

Received 5 December 2019; Received in revised form 21 May 2020; Accepted 30 June 2020

Available online 17 July 2020

1875-5100/© 2020 Elsevier B.V. All rights reserved.

**Table 1**  
Coal rank, maceral composition, and porosity analysis of the selected coal samples.

Sample No.	$R_o$ (%)	Maceral composition (%)				Proximate analysis (%)			
		V	I	E	M	$M_{ad}$	$A_d$	$V_d$	$FC_d$
#1	0.52	64.3	30.7	4.7	0.3	7.67	21.34	33.71	44.95
#2	0.63	75.6	22.7	0.3	0.4	12.68	3.52	25.81	71.04
#3	0.69	77.4	16.5	5.8	0.3	2.55	5.37	37.37	57.26
#4	0.71	65.6	34.0	0.3	0.1	7.36	1.15	27.81	71.04
#5	0.80	50.2	37.2	4.7	7.9	2.70	15.49	28.09	56.42
#6	1.19	54.0	38.4	0	7.6	0.88	7.84	21.97	70.19
#7	1.22	63.1	23.9	0	13.0	0.74	18.51	22.61	58.88
#8	1.32	53.7	37.5	0	8.8	0.98	14.54	19.92	65.54
#9	1.54	57.8	35.9	0	6.3	1.37	9.19	15.57	75.24
#10	1.64	81.4	15.6	0	3.0	0.88	6.76	16.83	76.41
#11	2.21	58.6	41.4	0	0	0.56	8.54	21.99	68.91
#12	2.36	80.3	10.7	1.0	8.0	0.24	7.20	7.39	87.21
#13	2.54	83.4	15.9	0	0.7	0.43	12.06	12.46	75.05
#14	2.95	90.4	8.4	1.0	0.2	0.34	10.67	13.16	77.17
#15	3.07	87.4	12.2	0.4	0.0	0.45	8.62	13.07	79.31

Notes:  $R_o$  = vitrinite reflectance under oil immersion. V = vitrinite; I = inertinite; E = exinite; M = minerals.  $M_{ad}$  = moisture (air-dried basis);  $A_d$  = ash (dry basis);  $V_d$  = volatile (dry, ash free basis);  $FC_d$  = carbon (air-dried basis).

characterization coal pores. For example, image analysis methods can only reflect the local information of pore structures (Nie et al., 2015; Liu and Wu, 2017). Gas adsorption method only can reflect the information of pores with diameter less than 200 nm, cannot finely characterize parts of macro-pores and fractures in coal (Hassan, 2012; Chen et al., 2018). While MIP measurement is generally used to analyze meso-pores and macro-pores because of the high pressure of intrusion mercury can destroy the micro-pore structure of coal (Friesen and Mikula, 1988; Yao and Liu, 2012; Li et al., 2015; Gao et al., 2018).

Recently, nuclear magnetic resonance (NMR) method serves as an accurate technique to evaluate petrophysical properties of porous medium, like wettability, PSD, permeability and so on (Al-Mahrooqi et al., 2006; Rezaee et al., 2012; Sulucarnain et al., 2012; Yao et al., 2014; Liang et al., 2019; Su et al., 2018; Li et al., 2019; Lyu et al., 2019). For example, Sun et al. (2018) investigated the wettability changed of CO<sub>2</sub>-water in coals by NMR measurement and found CO<sub>2</sub> can reduce the water wettability. An absolute and accurate PSD can be obtained from the NMR  $T_2$  distribution using centrifugal experiment method and surface relaxivity method (Saidian and Prasad, 2015; Zheng et al., 2019a, b). Based on the results of fully-saturated NMR  $T_2$  distribution, the pores in coal were classified into three types: adsorption-pore ( $T_2 < 2.5$  ms), seepage-pore ( $2.5 \text{ ms} < T_2 < 50$  ms) and fracture ( $T_2 > 100$  ms) (Yao et al., 2010). In addition, according to the shape of  $T_2$  spectra, the connectivity characteristics of rocks can also be estimated. Continuous  $T_2$  spectrum usually reflects good connectivity among different pores, whereas discontinuous  $T_2$  spectrum indicates the poor connectivity (Yao et al., 2010).

NMR  $T_2$  cutoff value ( $T_{2C}$ ), a key NMR measurement parameter that defined the movable and irreducible-water pore, and it is also an important determined parameter for evaluating permeability and full-scale PSD (Ge et al., 2015a, b; Xu et al., 2017). Conventionally, default values such as 33 and 90 ms are often chosen for sandstone and carbonate, respectively (Timur, 1969; Coates et al., 1999). However, unlike the conventional reservoirs, many researchers found that the  $T_{2C}$  of unconventional reservoirs shows a large deviation. For instance, Yao et al. (2010) determined the  $T_{2C}$  of coals range from 2.5 to 32 ms. Liu et al. (2018b) suggested the  $T_{2C}$  value in Lower Silurian Longmaxi shales in the range of 0.45–2.98 ms. Possibly because of the more complicated and heterogeneity pore structure characterization in coals and shales than those in conventional reservoirs.

For NMR pore size classification, the most commonly used method is dividing a fully-saturated  $T_2$  spectrum into two parts based on the determined  $T_{2C}$ :  $T_2 > T_{2C}$  for the free fluid parts corresponds to free fluid pores,  $T_2 < T_{2C}$  for the irreducible fluid parts corresponds to irreducible fluid pore (Ge et al., 2015a, b; Zhang et al., 2018). In this study, we

defined this pore classification standard as single  $T_2$  cutoffs model. However, when we tried to apply this model to distinguish the movable and irreducible fluid pores, we found that when  $T_2 > T_{2C}$ , there is still some irreducible fluid after high pressure centrifugal experiments. In addition, there is still some movable fluid when  $T_2 < T_{2C}$ . Thus, the pore classification determined by single  $T_2$  cutoffs model cannot accurately describe the pores with different fluid characteristics. Liu et al. (2018b) and Yuan et al. (2018) classified the shale pores into unrecoverable, capillary bound and movable fluid-pores based on dual  $T_2$  cutoffs which combined centrifugal and heat-treated measurements. However, the heat-treated experiments may destroy the organic matter in coals which cannot reflect the real coal PSDs. Fan et al. (2018) and Liu et al. (2018a) proposed a novel pore types classification in tight sandstones only depended on NMR centrifugal experiments, which divided the pores into absolute irreducible pores, absolute movable pores and partial movable pores. It should be noticed that the  $T_2$  distributions of coals usually characterized by a trio-modal, that are different from sandstones that having typical bimodal distribution in Fan et al. (2018) and Liu et al. (2018a). In this study, fifteen coal samples with different ranks were collected and performed for a series of NMR and centrifugal measurements. After that, the shortcomings of single  $T_2$  cutoffs model in pore fluid distinguishing were investigated. Finally, we introduced a novel method for accurate classification of pore fluid/size in coals.

## 2. Samples and experiments

### 2.1. Samples

Fifteen coal samples with the different coal ranks were collected from the Junngar basin and Qinshui basin. The basic information for those samples, including the mean maximum vitrinite reflectance ( $R_o$ ), coal maceral composition, and proximate analysis are listed in Table 1. The coals are subbituminous to anthracite, with a wide range of  $R_o$  from 0.52% to 3.07%. Vitrinite contents of coals vary from 50.2% to 90.4%, accounting for the largest proportion of maceral group composition. Proximate analyses are mainly characterized by variable carbon content (44.95%–87.21%), followed by volatile (7.39%–37.37%).

### 2.2. NMR and centrifugal experiments

Many previous studies have described the detailed principle of the NMR experiments (e.g. Yao et al., 2010; Ge et al., 2015b), here, we only present a brief review on NMR theory. For a typical  $T_2$  distribution, it can be affected by bulk relaxation ( $T_{2B}$ ), surface relaxation ( $T_{2S}$ ) and diffusion relaxation ( $T_{2D}$ ). In this study, the  $T_{2B}$  and  $T_{2D}$  can be ignored

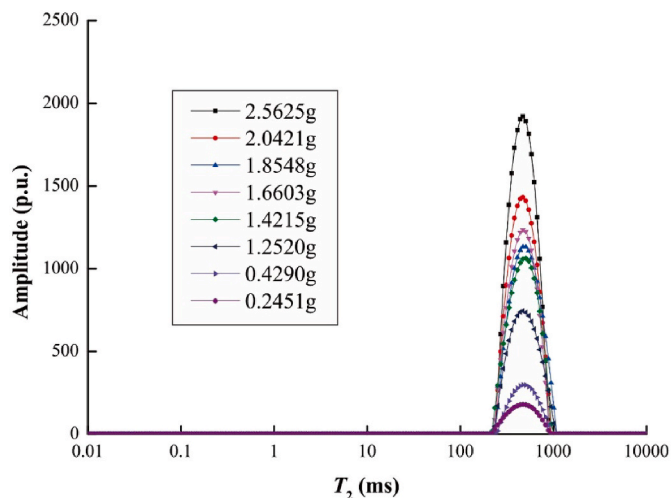


Fig. 1. NMR  $T_2$  distributions of bulk water with different masses.

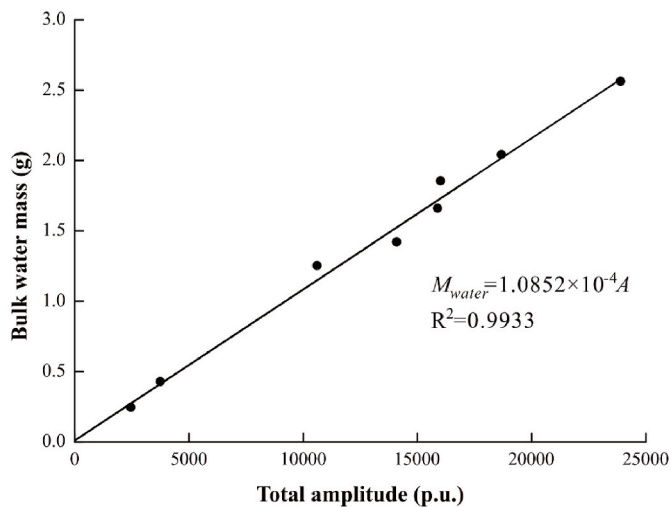


Fig. 2. Relationship between the total NMR  $T_2$  amplitude and bulk water mass.

by applying uniform magnetic field and CPMG sequence. Thus, the  $T_2$  relaxation time approximately equals to  $T_{2S}$ :

$$\frac{1}{T_2} \approx \frac{1}{T_{2S}} = \rho_2 \left( \frac{S}{V} \right) \quad (1)$$

where  $\rho_2$  is surface relaxivity; and  $S/V$  is the pore surface to volume ratio.

Prior to NMR and centrifugal measurements, each coal sample was drilled as a coal plug with 2.5 cm diameter and 5.0 cm length. Using the same coal sample, a series of NMR and centrifugal experiments were conducted. In this work, the NMR testing parameter were set up the same as Zheng et al. (2019a) by using Suzhou Niumag MiniMR60 analytical instrument (magnetic strength of 0.5 T). The workflow of the experiments was shown as following: 1) these plug samples were dried to remove the remaining fluids using a drying oven at 95 °C for 24 h, 2) all samples are fully saturated deionized water in a pressure-saturated container for 12 h at 15 MPa confining pressure, 3) fully water-saturated samples were packed by non-magnetic film, to be measured for NMR, and 4) these samples were centrifuged on an increasing centrifugal pressure of 0.69, 0.92, 1.15, 1.38 and 1.61 MPa, corresponding to centrifugal rotate speeds of 3000, 4000, 5000, 6000 and 7000 rpm, respectively, under the laboratory temperature (293 K) and humidity (32%). Finally, the  $T_2$  spectra at different centrifugal

pressures were recorded.

### 3. Results and discussions

#### 3.1. Relaxation properties of bulk water

To analyze the properties of fluid in coals by NMR measurement, the first and indispensable step is to establish a model for quantity characterization of water based on the NMR data. Fig. 1 shows the results of NMR  $T_2$  distributions for different masses bulk water. The NMR  $T_2$  spectra exhibits a clear peak, with a long relaxation time at approximately 200–1000 ms. As shown in Fig. 2, it can be found that the NMR spectra amplitude shows an evident linear relationship with bulk water mass,

$$M_{water} = 1.0852 \times 10^{-4} A \quad (R^2 = 0.9933) \quad (2)$$

where  $M_{water}$  is the mass of distilled water with units of g,  $A$  (dimensionless) means the amplitude of measured NMR  $T_2$  spectra.

#### 3.2. Relaxation properties of samples with fully saturated water and after centrifuge experiment

Fig. 3 shows the results of NMR  $T_2$  distribution for the fully saturated coals and after centrifugal experiments. The  $T_2$  distribution of coals at fully saturated conditions are shown as blue lines in Fig. 3, which exhibit an evident multimodal distribution. The first dominant peak occurs at approximately 0.01–8 ms, with a slow relaxation property, indicating the characteristics of smaller pores in coals. The second peak is found between 10 and 100 ms, that corresponds to the larger pores in coals. For most of samples (except for sample #7) existing a third peak, with a fast relaxation property at >100 ms. That illustrates the fractures are well developed in these coals. Based on the NMR amplitude of coal samples under fully saturated condition and equation (2), the total NMR porosity ( $\phi_{NMR}$ ) were obtained. Taken the sample #1 as an example, the total  $T_2$  amplitude under fully-saturated condition is 11652 (p.u.) (Table 2), corresponding to 1.2645 g water saturated in coal pore system based on equation (2). The volume of the coal plug is 24.53 cm<sup>3</sup> (size of 2.5 diameter and 5.0 cm length), thus, the NMR porosity for sample #1 is 5.16% – water volume divided by sample volume. The calculated values of  $\phi_{NMR}$  for all coals range from 3.13 to 12.24% (Table 2).

With the increasing centrifugal pressures, the first dominant peak shows a slight decreasing trend for most coals (except for the sample #4 and #14). It should be noticed that the first peak of sample #4 and #14 exhibits a slight increase trend after 0.62 MPa and 0.92 MPa centrifugal experiments. This may because of the complicated pore morphology and spontaneous imbibition within micro-pores. While for the second and third peak, there is an evident reduction for all coal samples, that is the result of some movable fluids in coal pore-fracture system are centrifuged by centrifugal treatments.

#### 3.3. Single $T_2$ cutoffs model

Previous studies (Ge et al., 2015b; Xu et al., 2017) have found that there was a single  $T_2$  cutoff value (denoted as  $T_{2C}$ ) can be calculated by combining NMR and centrifugal experiments. Based on this calculated  $T_{2C}$ , the pore fluids of rocks are classified into movable fluid part ( $T_2 > T_{2C}$ ), and irreducible fluid part ( $T_2 < T_{2C}$ ). Here, we defined this pore fluid classification standard as single  $T_2$  cutoffs model. In this section, we calculated the values of  $T_{2C}$  for all coal samples and discussed the limitations of the single  $T_2$  cutoffs model.

##### 3.3.1. Determination of $T_{2C}$

To calculate the values of  $T_{2C}$ , the first step is to determine the optimal centrifugal pressure based on the NMR results of different pressures centrifugal experiment. Fig. 4 and Table 3 show the water

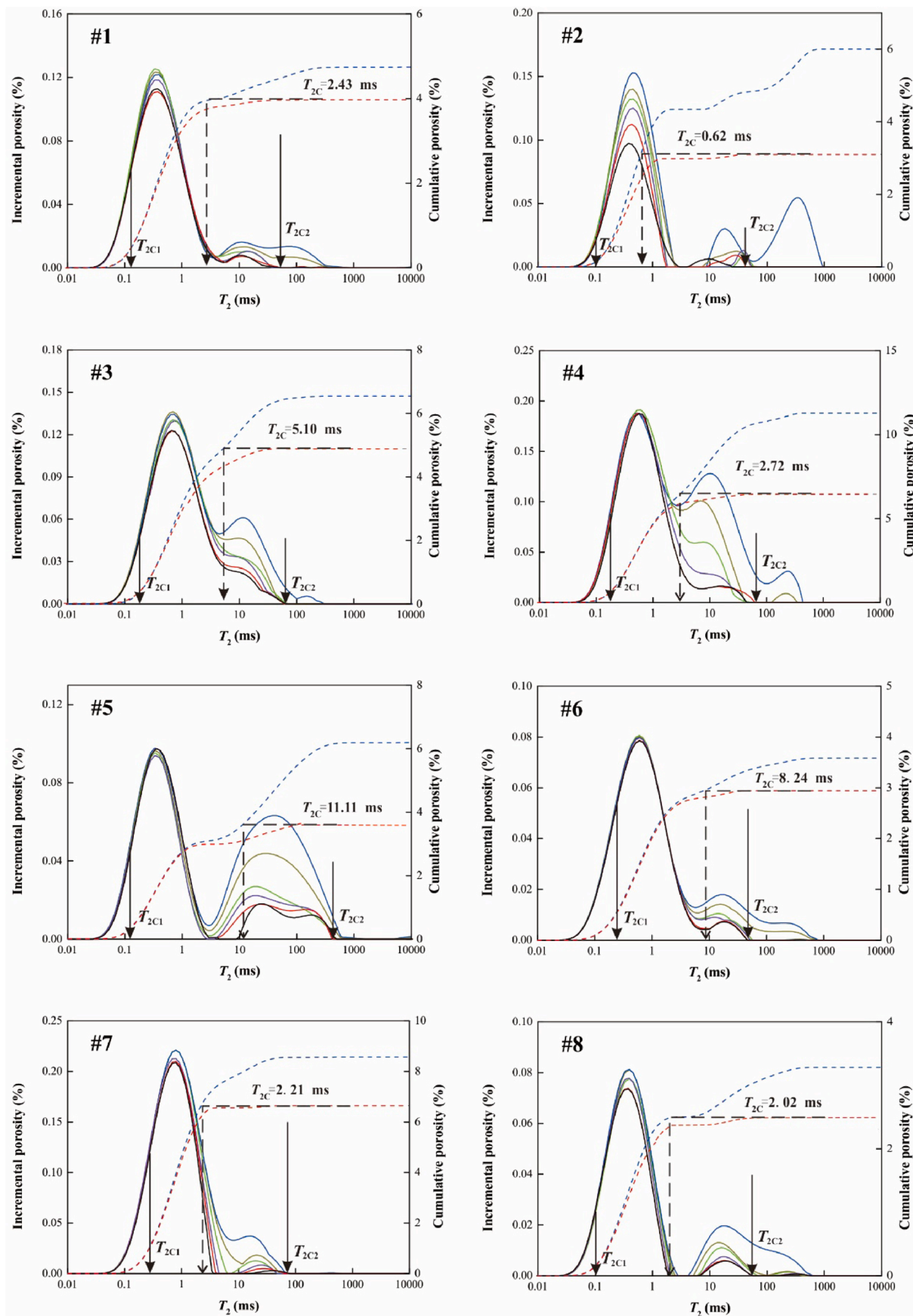


Fig. 3. The single  $T_2$  cutoffs and dual  $T_2$  cutoffs determination by the NMR centrifugal experiments (to be continued).

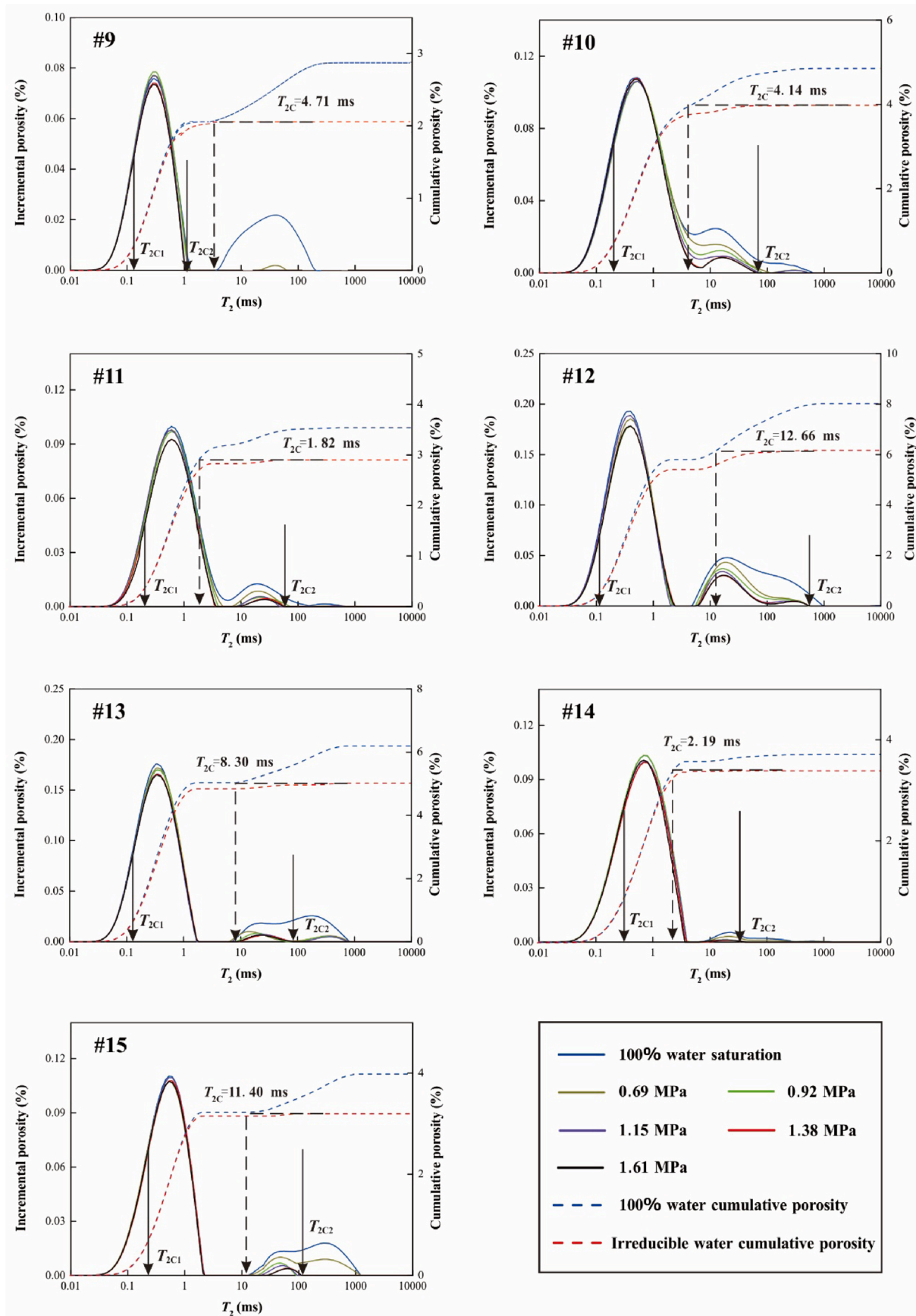


Fig. 3. (continued).

**Table 2**  
NMR single  $T_2$  cutoffs, dual  $T_2$  cutoffs, fully-saturated coal amplitude and porosity of coal samples.

Sample No.	Fully-saturated coal amplitude (p.u.)	$\phi$ NMR (%)	Single $T_2$ cutoffs model			Dual $T_2$ cutoffs model				
			$T_{2C}$ (ms)	$\phi$ -movable (%)	$\phi$ -irreducible (%)	$T_{2C1}$ (ms)	$T_{2C2}$ (ms)	$\phi_1$ (%)	$\phi_2$ (%)	$\phi_3$ (%)
#1	11652	5.15	2.43	0.85	4.30	0.16	36.12	0.76	4.02	0.37
#2	14718	6.51	0.62	3.16	3.35	0.10	41.50	0.17	5.06	1.28
#3	16043	7.10	5.10	1.79	5.31	0.17	62.95	0.36	6.63	0.11
#4	27670	12.24	2.72	5.23	7.01	0.18	72.33	0.75	10.87	0.62
#5	15184	6.72	11.11	2.56	4.16	0.15	439.76	0.55	6.13	0.04
#6	8782	3.89	8.24	0.70	3.19	0.34	58.73	0.96	2.71	0.22
#7	20998	9.29	2.21	2.08	7.21	0.32	67.48	1.49	7.79	0.01
#8	8046	3.60	2.02	0.95	2.65	0.15	54.79	0.42	2.9	0.28
#9	7065	3.13	4.71	1.04	2.09	0.13	1.05	0.38	1.85	0.9
#10	11897	5.26	4.14	0.94	4.32	0.18	83.10	0.68	4.46	0.12
#11	8684	3.84	1.82	0.68	3.16	0.14	58.72	0.16	3.63	0.05
#12	19673	8.70	12.66	2.01	6.69	0.14	89.07	0.88	7.07	0.75
#13	15184	6.72	8.30	1.05	5.67	0.15	77.53	0.96	5.08	0.68
#14	9101	4.03	2.19	0.36	3.67	0.23	41.50	0.6	3.37	0.06
#15	9763	4.32	11.40	0.74	3.58	0.21	109.70	0.66	3.17	0.49

Notes:  $\phi_1$ ,  $\phi_2$  and  $\phi_3$  is absolute irreducible porosity, partial movable porosity and absolute movable porosity, respectively.

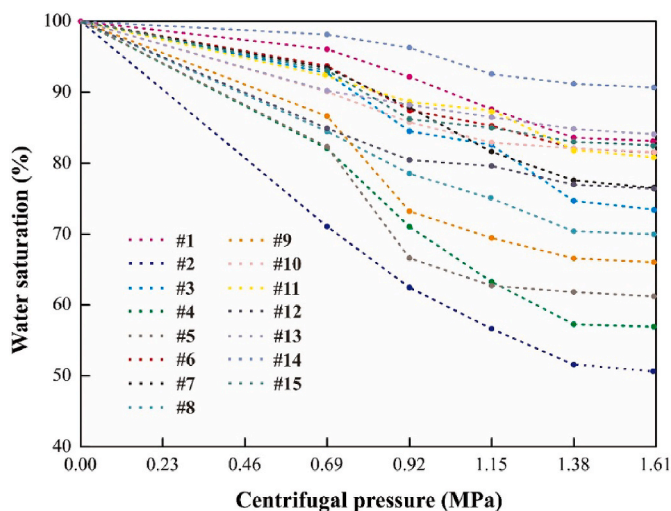


Fig. 4. Variation characteristics of water saturation in coals.

**Table 3**  
Water saturation of coals under different centrifugal pressures.

Sample No.	Water saturation under different centrifugal pressures				
	0.69 MPa (%)	0.92 MPa (%)	1.15 MPa (%)	1.38 MPa (%)	1.61 MPa (%)
#1	96.08	92.16	87.61	83.62	83.11
#2	71.06	62.48	56.64	51.58	51.24
#3	92.68	84.51	82.55	74.7	74.21
#4	82.06	71.03	63.28	57.27	56.91
#5	82.3	66.61	65.71	61.85	61.25
#6	93.73	87.46	85.30	82.11	81.50
#7	93.43	87.85	81.62	77.56	76.87
#8	84.48	78.50	75.02	70.39	69.94
#9	86.61	73.22	69.44	66.56	66.02
#10	90.05	85.77	83.90	82.11	81.58
#11	92.28	88.63	87.42	81.90	81.31
#12	84.91	80.45	79.60	76.96	76.42
#13	90.22	88.23	86.49	84.82	84.05
#14	98.14	96.28	92.55	91.18	90.66
#15	93.1	86.19	85.02	83.02	82.51

saturation after centrifugal experiments for the studied plugs. As the centrifugal pressure increased from 0.69 MPa to 1.38 MPa, the water saturation results exhibit an evident downward trend. The relative error of water saturation after 1.15 MPa and 1.38 MPa centrifugal

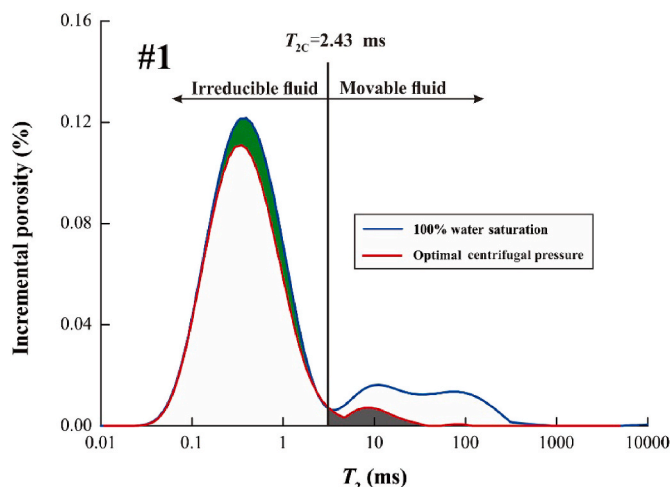


Fig. 5. Single  $T_2$  cutoffs model for the coal sample #1.

experiments for all coals in the range of 1.48–9.51%, averaging at ~5.0%. While the water saturation relative errors between 1.38 MPa and 1.61 MPa centrifugal pressures are less than 1.0%. We assumed the optimal numerical relative error index for determination optimal centrifugal pressure is 1.0%. Thus, the optimal centrifugal pressure to determinate  $T_{2C}$  in this study is 1.38 MPa.

As shown in Fig. 5, in order to convenient and clearly calculate the  $T_{2C}$  values, we only selected fully saturated and 1.38 MPa centrifugal NMR  $T_2$  distributions in Fig. 3. The method for determination  $T_{2C}$  by centrifugal experiments were detailed in Yao et al. (2010). First, the two NMR  $T_2$  distributions under fully water-saturated condition and those after 1.38 MPa centrifugal experiments are transformed into two accumulative  $T_2$  curves (blue and red dotted line), respectively. Then, the horizontal line from the 1.38 MPa centrifugation cumulative  $T_2$  curve is drawn and intersects with fully water-saturated cumulative  $T_2$  curve at one point. Finally, the vertical line from this intersection point is drawn, intersecting with the X-axis which corresponds to the value of  $T_{2C}$ . In this study, the calculated  $T_{2C}$  in the range of 0.62–12.66 ms for all selected coals (Table 2), which shows a wider deviation than the values of shales (0.45–2.98 ms) calculated in Liu et al. (2018b).

### 3.3.2. Limitation in the application of single $T_2$ cutoffs model

One of the most important application of  $T_{2C}$  is to distinguish the movable fluid and irreducible fluid. Conventionally, based on the values of  $T_{2C}$ , the NMR  $T_2$  spectrum of a sample with fully saturated condition

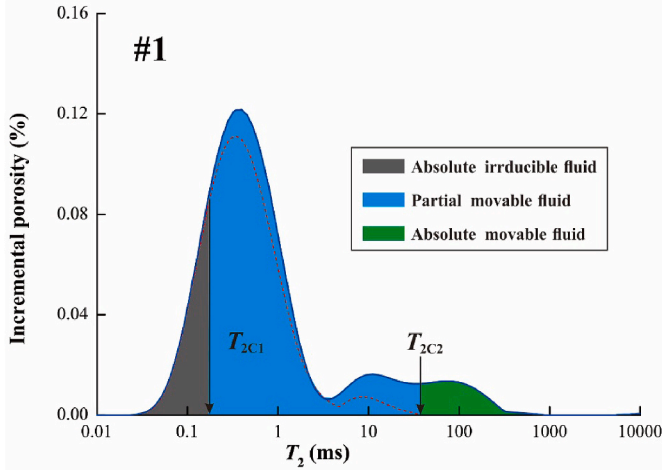


Fig. 6. Dual  $T_2$  cutoffs model for the coal sample #1.

can be divided into two parts: the  $T_2 < T_{2C}$  for the irreducible fluid, and the  $T_2 > T_{2C}$  for the movable fluid. In this study, when we tried to divide the coal reservoir fluid into irreducible fluid and movable fluid based on the  $T_{2C}$ , we found that it has some shortcomings in accurate quantitative characterization of different type pore fluids in coals.

Here, the coal sample #1 was taken as an example to illustrate the limitation of the single  $T_2$  cutoffs model in typing movable and irreducible fluid. As shown in Fig. 5, it is easily to find that when  $T_2 > T_{2C}$ , there is still some irreducible fluid after high pressure centrifugal experiments (gray region in Fig. 5). It may be the result of there are still some fluids remained in the larger pores as a form of thin film, since the development of hydrophilic mineral in the surface of pores. Moreover, there are still some movable fluids when  $T_2 < T_{2C}$  (green region in Fig. 5). Following the above observations, we can find that the single  $T_2$  cutoffs model cannot distinguish the different types of fluids in coals accurately. Hence, a new model is needed to overcome the shortcoming of single  $T_2$  cutoffs model, and to advance quantitative characterization of different types pore fluid.

### 3.4. Dual $T_2$ cutoffs model

As discussed, the single  $T_2$  cutoffs model cannot be accurately used to distinguish the different types of fluids in coals. In this section, a new model was introduced to accurate quantitative characterization of different pore fluids in coals determined from the perspective of NMR and centrifugal testing, that is dual  $T_2$  cutoffs model.

#### 3.4.1. The principle of dual $T_2$ cutoffs model

As shown in Fig. 6, the coal sample #1 was taken as an example to illustrate the dual  $T_2$  cutoffs model. These pore fluids in coals were re-classified into three types (absolute irreducible fluid, absolute movable fluid and partial movable fluid) rather than two commonly types (irreducible and movable fluid). For the absolute irreducible fluid (gray region in Fig. 6), the NMR  $T_2$  spectra show almost no changes between the fully water-saturated and those after centrifugal experiments, which indicates the behavior of this part fluids are absolute irreducible. The transverse relaxation time boundary between the absolute irreducible fluid and partial movable fluid was denoted as  $T_{2C1}$ . It should be noticed that the NMR  $T_2$  spectra of fully water-saturated and those may not extremely coincide in absolute irreducible fluid part for some samples. Here, the principle of  $T_{2C1}$  determination was expressed as following:

$$\frac{A_{Fully, T_i} - A_{Centrifugal, T_i}}{A_{Fully, T_i}} > 0.01 \quad (3)$$

where  $A_{Fully, T_i}$  and  $A_{Centrifugal, T_i}$  is the NMR amplitude under fully water-saturated, after centrifugal condition at  $T_i$ , respectively. The minimum of  $T_i$  that meets the conditions of Eq. (3) corresponding to  $T_{2C1}$ .

For the absolute movable fluid (green region in Fig. 6), the NMR  $T_2$  distributions of the fluids complete disappeared after centrifugal experiments, and we defined the transverse relaxation time boundary between the absolute movable fluid and partial movable fluid as the  $T_{2C2}$ . For the partial movable fluid (blue region in Fig. 6), we can find that the  $T_2$  distributions of  $T_{2C1} < T_2 < T_{2C2}$  show an evident reduction after centrifugal experiments rather than complete remove, and we defined as this part of fluid as the partial movable fluids.

#### 3.4.2. Determination of $T_{2C1}$ and $T_{2C2}$

According to the above principle of dual  $T_2$  cutoffs model, we calculated the  $T_{2C1}$  and  $T_{2C2}$  for all selected coal samples (see results in Fig. 3 and Table 2). In this study, the values of  $T_{2C1}$  ranges from 0.10 to 0.34 ms, while the  $T_{2C2}$  has a wider range from 1.05 ms to 439.76 ms.

Based on the calculated  $T_{2C1}$  and  $T_{2C2}$ , a fully saturated NMR  $T_2$  spectra of sample can be divided into three parts:  $T_2 < T_{2C1}$  for the absolute irreducible fluid parts,  $T_{2C1} < T_2 < T_{2C2}$  for the partial movable fluid parts and  $T_{2C2} < T_2$  for the absolute movable fluid parts. Moreover, the NMR total porosity ( $\phi_{NMR}$ ) of a coal sample can also be divided into three parts corresponds to the three types of pore fluids, which is absolute irreducible porosity (denoted as  $\phi_1$ ), partial movable porosity (denoted as  $\phi_2$ ), and absolute movable porosity (denoted as  $\phi_3$ ), respectively. The values of the  $\phi_1$ ,  $\phi_2$  and  $\phi_3$  can be calculated as follows:

$$\phi_1 = \frac{\int_{T_{min}}^{T_{2C1}} T_2 dT}{\int_{T_{min}}^{T_{max}} T_2 dT} \times \phi_{NMR} \quad (4)$$

$$\phi_2 = \frac{\int_{T_{2C1}}^{T_{2C2}} T_2 dT}{\int_{T_{min}}^{T_{max}} T_2 dT} \times \phi_{NMR} \quad (5)$$

$$\phi_3 = \frac{\int_{T_{2C2}}^{T_{max}} T_2 dT}{\int_{T_{min}}^{T_{max}} T_2 dT} \times \phi_{NMR} \quad (6)$$

where  $T_{min}$  is 0.01 ms;  $T_{max}$  is 10000 ms;  $T_{2C1}$  is the  $T_2$  cutoff between absolute irreducible and partial movable fluids, and  $T_{2C2}$  is the  $T_2$  cutoff between partial movable and absolute movable fluid;  $\phi_{NMR}$  is the total porosity measured by NMR experiments.

The calculated  $\phi_1$ ,  $\phi_2$  and  $\phi_3$  for all selected coals are shown in Table 2. Values of  $\phi_1$ ,  $\phi_2$  and  $\phi_3$  are in the range of 0.16–1.49% (average at 0.65%), 1.85–10.87% (average at 4.98%), and 0.01–1.28% (average at 0.40%), respectively. Of the three porosities,  $\phi_2$  accounts for largest proportion of the total porosity, secondly is  $\phi_1$ , and  $\phi_3$  contributes the lowest proportion.

### 3.5. NMR full-scale PSD

The NMR spectra with fully saturated conditions only can provide  $T_2$  distributions rather than the absolute full-scale PSD. There are two commonly used methods to acquire the full-scale PSD based on NMR measurement. One is centrifugal experiment method, the other is surface relaxivity method.

For the centrifugal experiment method, three steps should be performed to acquire the full-scale PSD that can be found in Yao et al. (2010). The first step is to determine an optimal centrifugal pressure and the values of  $T_{2C}$  by a series of centrifugal experiments. Then, the second step is to calculate the pore radius ( $r$ ) corresponding to the determined optimal centrifugal pressure based on Washburn equation. At last, the full-scale PSD is determined based on the relationship of any transverse relaxation time ( $T_{2i}$ ) and pore radius ( $r_{ci}$ ) that is the  $r_{ci} = \frac{r T_{2i}}{T_{2C}}$ . It should be noticed that the determined  $T_{2C}$  is not an accurate and absolute value, since there are still some movable fluids when  $T_2 < T_{2C}$ . Thus, the

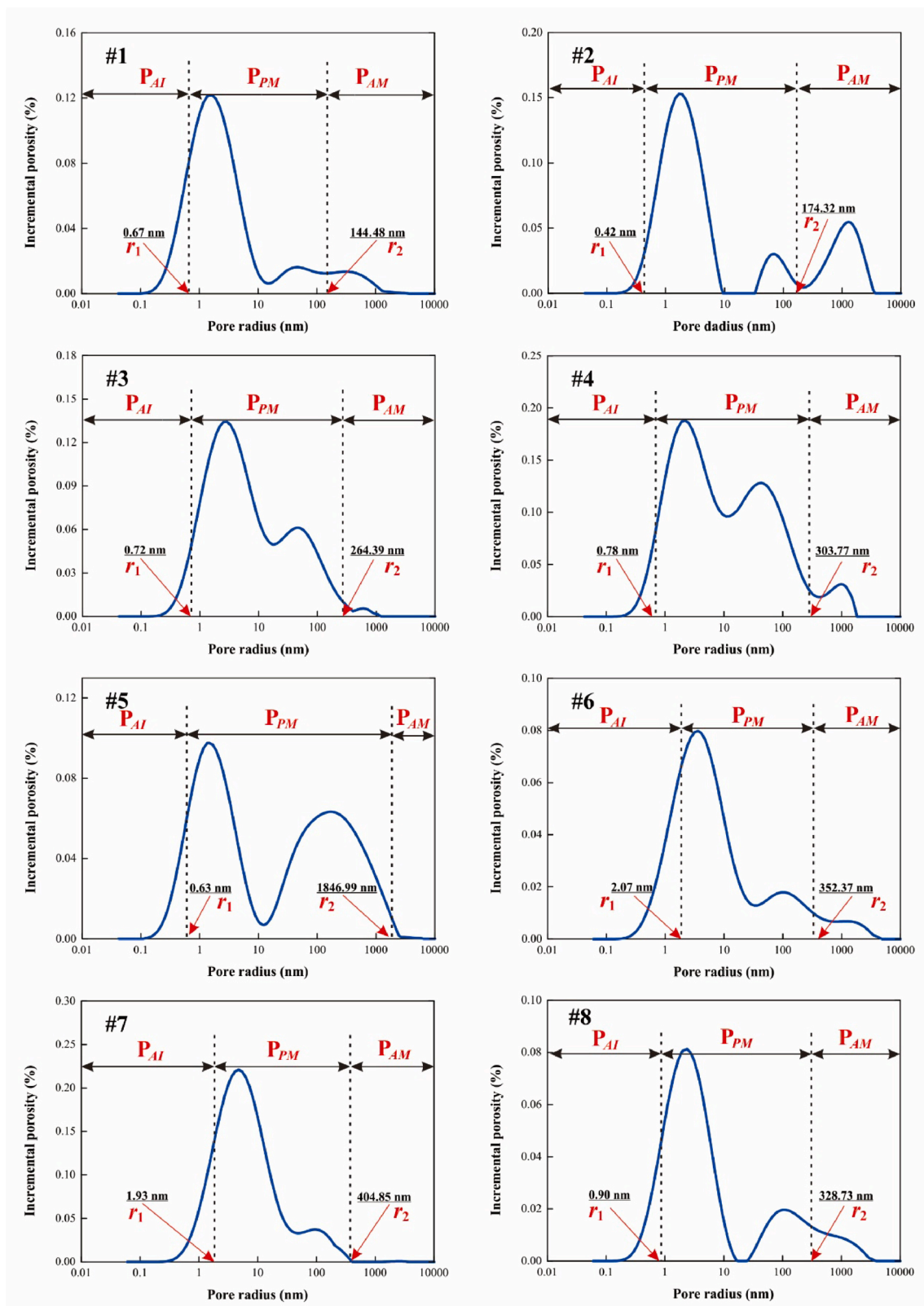


Fig. 7. PSDs and pore size classification of the selected coal samples (to be continued).

full-scale PSD determined by the centrifugal experiment method is inapplicable.

For the surface relaxivity method, Zheng et al. (2019) proposed a novel method for calculation surface relaxivity of coals by combining

low-temperature nitrogen adsorption (LTNA) and mercury intrusion porosimetry (MIP), and provided the references of surface relaxivity for different coals. They suggested 2.1  $\mu\text{m/s}$ , 3.0  $\mu\text{m/s}$  and 1.6  $\mu\text{m/s}$  for the surface relaxivity of low-, medium-, and high-rank coal. According to the

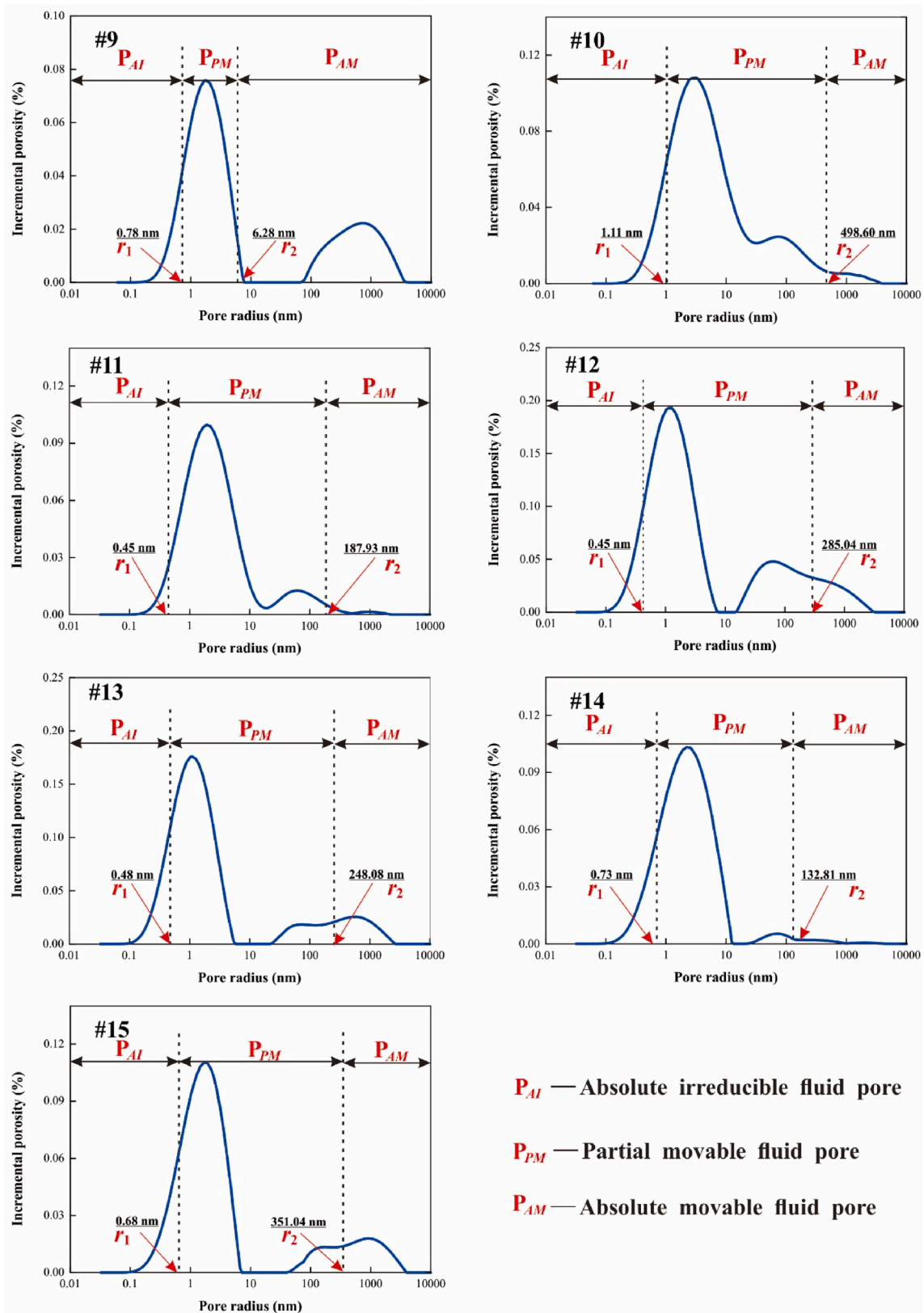


Fig. 7. (continued).

references of surface relaxivity in Zheng et al. (2019), the full-scale PSD in this study were obtained (Fig. 7).

As shown in Fig. 7, based on the dual  $T_2$  cutoffs model, the PSD of coals were reclassified into three types: absolute irreducible fluid pores

( $r < r_1$ ), partial movable fluid pores ( $r_1 < r < r_2$ ) and absolute movable fluid pores ( $r_2 < r$ ). Noted that  $r_1$  is the threshold pore radius of absolute irreducible fluid pores corresponding to  $T_{2C1}$ ,  $r_2$  is the threshold pore radius of absolute movable fluid pores corresponding to  $T_{2C2}$ . As shown

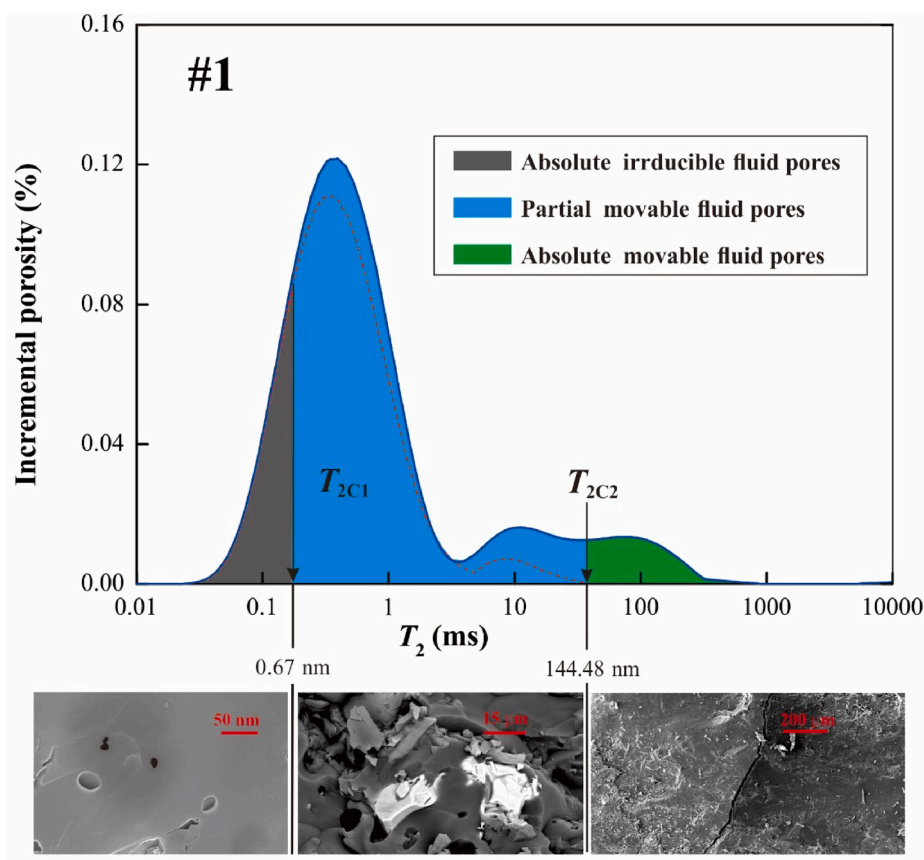


Fig. 8. Petrophysical dual  $T_2$  cutoffs model for sample #1.

in Fig. 7,  $r_1$  commonly have very low values in the range of 0.42–2.07 nm, while  $r_2$  ranges from 6.28 nm to 1846.99 nm.

Taking the sample #1 as example, the full-scale PSD classification petrological model that derived from the dual  $T_2$  cutoffs model was elucidated (Fig. 8). As shown in Fig. 8, the absolute irreducible fluid pores, partial movable fluid pores, and absolute movable fluid pores are in the radius of  $<0.67$  nm,  $0.67$  nm– $144.48$  nm, and  $>144.48$  nm, respectively. The absolute irreducible fluid pores are commonly developed in coal matrix and contribute little to fluid transportation, and the partial movable fluid pores mainly developed in mesopores, such as gas pores and tissue pores. The absolute movable fluid pores are usually related to fractures, that is good for pore fluid migration.

#### 4. Conclusions

This paper presented a significant model for pore fluid type and PSD classification in coals by combining NMR and centrifugal experiments. The main conclusions are as follows:

- (1) Based on NMR and centrifugal experiments, the  $T_{2C}$  of coals determined by the single  $T_2$  cutoff model in the range of 0.62–12.66 ms. When  $T_2 > T_{2C}$ , there is remaining some irreducible fluid in pores. There are still some movable fluids in pores when  $T_2 < T_{2C}$ , which indicates the single NMR  $T_2$  cutoffs model has some obvious shortcomings in pore fluid classification.
- (2) An effective method was proposed for pore fluid typing classification of coals denoted as the dual  $T_2$  cutoffs model. For a typical  $T_2$  spectrum with fully-saturated condition, the pore fluid of coals was re-classified into absolute movable fluid ( $T_2 > T_{2C2}$ ), partial movable fluid ( $T_{2C1} < T_2 < T_{2C2}$ ), and absolute irreducible fluid ( $T_{2C1} > T_2$ ). For all coal samples, the  $T_{2C1}$  ranges from 0.10 to 1.32 ms, while  $T_{2C2}$  in the range of 36.12–89.07 ms.

- (3) Based on dual  $T_2$  cutoffs model, a conceptual model were proposed to clarify a full-scale PSD classification: absolute irreducible fluid pores, partial movable fluid pores and absolute movable fluid pores.

#### Declaration of competing interest

The authors declare that they have no known competing financial interests or personal relationships that could have appeared to influence the work reported in this paper.

#### CRediT authorship contribution statement

**Sijian Zheng:** Validation, Writing - original draft, Investigation. **Yanbin Yao:** Conceptualization, Methodology, Supervision, Project administration, Funding acquisition. **Derek Elsworth:** Writing - review & editing. **Bo Wang:** Resources. **Yong Liu:** Formal analysis.

#### Acknowledgments

We acknowledge financial support from the National Natural Science Foundation of China (41830427; 41872123), the National Major Science and Technology Projects of China (2016ZX05043-001), the Key research and development project of Xinjiang Uygur Autonomous Region (2017B03019-1), and the Fundamental Research Funds for the Central Universities (292019252).

#### Appendix A. Supplementary data

Supplementary data to this article can be found online at <https://doi.org/10.1016/j.jngse.2020.103466>.

## References

- Al-Mahrooqi, S.H., Grattoni, C.A., Muggeridge, A.H., Zimmerman, R.W., Jing, X.D., 2006. Pore-scale modelling of NMR relaxation for the characterization of wettability. *J. Petrol. Sci. Eng.* 52, 172–186.
- Chen, Y.L., Qin, Y., Wei, C.T., Huang, L.L., Shi, Q.M., Wu, C.F., Zhang, X.Y., 2018. Porosity changes in progressively pulverized anthracite subsamples: implications for the study of closed pore distribution in coals. *Fuel* 225, 612–622.
- Clarkson, C.R., Bustin, R.M., 1999. The effect of pore structure and gas pressure upon the transport properties of coal: a laboratory modeling study. 2. Adsorption rate modeling. *Fuel* 78, 1345–1362.
- Close, J.C., 1993. Natural fracture in coal. In: Law, B.E., Rice, D.D. (Eds.), *Hydrocarbons from Coal*, vol. 38. AAPG, p. 119–132.
- Coates, G.R., Xiao, L.Z., Primmer, M.G., 1999. *NMR Logging Principles and Applications*. Gulf Publishing Company.
- Du, Y., Sang, S.X., Pan, Z.J., Wang, W.F., Liu, S.Q., Fu, C.Q., Zhao, Y.C., Zhang, J.Y., 2019. Experimental study of supercritical CO<sub>2</sub>-H<sub>2</sub>O-coal interactions and the effect on coal permeability. *Fuel* 253, 369–382.
- Fan, Y.R., Liu, J.Y., Ge, X.M., Deng, S.G., Liu, H.L., Gu, D.N., 2018. Permeability evaluation of tight sandstone based on dual T<sub>2</sub> cutoff values measured by NMR. *Chin. J. Geophys.* 61 (4), 1628–1638.
- Friesen, W.I., Mikula, R.J., 1988. Mercury porosimetry of coals-pore volume distribution and compressibility. *Fuel* 67, 1516–1520.
- Gao, F.L., Song, Y., Li, Z., Xiong, F.Y., Chen, L., Zhang, X.X., Chen, Z.Y., Moortgat, J., 2018. Quantitative characterization of pore connectivity using NMR and MIP: a case study of the Wangyinpu and Guanyintang shales in the Xiuyu basin, Southern China. *Int. J. Coal Geol.* 197, 53–65.
- Ge, X.M., Fan, Y.R., Li, J.T., Zahid, M.A., 2015a. Pore structure characterization and classification using multifractal theory-An application in Santanghu Basin of western China. *J. Petrol. Sci. Eng.* 127, 297–304.
- Ge, X.M., Fan, Y.R., Zhu, X.J., Chen, Y.G., Li, R.Z., 2015b. Determination of nuclear magnetic resonance T<sub>2</sub> cutoff value based on multifractal theory-An application in sandstone with complex pore structure. *Geophysics* 80 (1), 11–21.
- Hassan, J., 2012. Pore size distribution calculation from <sup>1</sup>H NMR signal and N<sub>2</sub> adsorption-desorption techniques. *Physica B* 407, 3797–3801.
- Karacan, C.O., Ruiz, F.A., Cotè, M., Phipps, S., 2011. Coal mine methane: a review of capture and utilization practices with benefits to mining safety and to greenhouse gas reduction. *Int. J. Coal Geol.* 86, 121–156.
- Li, W., Liu, H.F., Song, X.X., 2015. Multifractal analysis of Hg pore size distributions of tectonically deformed coals. *Int. J. Coal Geol.* 145, 138–152.
- Li, X., Fu, X.H., Ranjith, P.G., Xu, J., 2019. Stress sensitivity of medium- and high volatile bituminous coal: an experimental study based on nuclear magnetic resonance and permeability-porosity tests. *J. Petrol. Sci. Eng.* 172, 889–910.
- Liang, C., Xiao, L.Z., Zhou, C.C., Wang, H., Hu, F.L., Liao, G.Z., Ji, Z.J., Liu, H.B., 2019. Wettability characterization of low-permeability reservoirs using nuclear magnetic resonance: an experimental study. *J. Petrol. Sci. Eng.* 178, 121–132.
- Liu, J.Y., Fan, Y.R., Ge, X.M., Wu, F., 2018a. Permeability estimation of tight sandstone based on dual T<sub>2</sub> cutoff value model and fluid substitution. In: 80th EAGE Conference and Exhibition 2018.
- Liu, X.L., Wu, C.F., 2017. Simulation of dynamic changes of methane state based on NMR during coalbed methane output. *Fuel* 194, 188–194.
- Liu, Y., Yao, Y.B., Liu, D.M., Zheng, S.J., Sun, G.X., Chang, Y.H., 2018b. Shale pore size classification: an NMR fluid typing method. *Mar. Petrol. Geol.* 96, 591–601.
- Lyu, C.H., Ning, Z.F., Chen, M.Q., Wang, Q., 2019. Experimental study of boundary condition effects on spontaneous imbibition in tight sandstones. *Fuel* 235, 374–383.
- Moore, T.A., 2012. Coalbed methane: a review. *Int. J. Coal Geol.* 101, 36–81.
- Nie, B.S., Liu, X.F., Yang, L.L., Meng, J.Q., Li, X.C., 2015. Pore structure characterization of different rank coals using gas adsorption and scanning electron microscopy. *Fuel* 158, 908–917.
- Rezaee, R., Saeedi, A., Clennell, B., 2012. Tight gas sands permeability estimation from mercury injection capillary pressure and nuclear magnetic resonance data. *J. Petrol. Sci. Eng.* 92–99, 88–89.
- Saidian, M., Prasad, M., 2015. Effect of mineralogy on nuclear magnetic resonance surface relaxivity: a case study of Middle Bakken and Three Forks formations. *Fuel* 161, 197–206.
- Su, S.Y., Jiang, Z.X., Shan, X.L., Zhu, Y.F., Wang, P., Luo, X., Li, Z., Zhu, R.F., Wang, X.Y., 2018. The wettability of shale by NMR measurements and its controlling factors. *J. Petrol. Sci. Eng.* 169, 309–316.
- Sulucarnain, I.D., Sondergeld, C.H., Rai, C.S., 2012. An NMR Study of Shale Wettability and Effective Surface Relaxivity, SPE Canadian Unconventional Resources Conference. Society of Petroleum Engineers, Calgary, Alberta, Canada.
- Sun, X.X., Yao, Y.B., Liu, D.M., Zhou, Y., 2018. Investigations of CO<sub>2</sub>-water wettability of coal: NMR relaxation method. *Int. J. Coal Geol.* 188, 38–50.
- Timur, A., 1969. Pulsed nuclear magnetic resonance studies of porosity, movable fluid and permeability of sandstones. *J. Petrol. Technol.* 6, 775–786.
- Weniger, P., Francù, J., Hemza, P., Krooss, B.M., 2012. Investigations on the methane and carbon dioxide sorption capacity of coals from the SW upper Silesian Coal Basin Czech Republic. *Int. J. Coal Geol.* 93, 23–39.
- Xu, J.Z., Zhai, C., Liu, S.M., Qin, L., Wu, S.J., 2017. Pore variation of three different metamorphic coals by multiple freezing-thawing cycles of liquid CO<sub>2</sub> injection for coalbed methane recovery. *Fuel* 28 (6), 41–51.
- Yao, Y.B., Liu, D.M., 2012. Comparison of low-field NMR and mercury intrusion porosimetry in characterizing pore size distributions of coals. *Fuel* 95, 152–158.
- Yao, Y.B., Liu, D.M., Che, Y., Tang, D.Z., Tang, S.H., Huang, W.H., 2010. Petrophysical characterization of coals by low-field nuclear magnetic resonance (NMR). *Fuel* 89, 1371–1380.
- Yao, Y.B., Liu, D.M., Xie, S.B., 2014. Quantitative characterization of methane adsorption on coal using a low-field NMR relaxation method. *Int. J. Coal Geol.* 131, 32–40.
- Yao, Y.B., Liu, J., Liu, D., Chen, J., Pan, Z.J., 2019. A new application of NMR in characterization of multiphase methane and adsorption capacity of shale. *Int. J. Coal Geol.* 201, 76–85.
- Yuan, Y.J., Rezaee, R., Verrall, M., Hu, S.Y., Zou, J., Testmanti, Nadia, 2018. Pore characterization and clay bound water assessment in shale with a combination of NMR and low-pressure nitrogen gas adsorption. *Int. J. Coal Geol.* 194, 11–21.
- Zhang, P.F., Lu, S.F., Li, J.Q., Chen, C., Xue, H.T., Zhang, J., 2018. Petrophysical characterization of oil-bearing shales by low-field nuclear magnetic resonance (NMR). *Mar. Petrol. Geol.* 89, 775–785.
- Zhao, Y.X., Sun, Y.F., Liu, S.M., Wang, K., Jiang, Y.D., 2017. Pore structure characterization of coal by NMR cryoporometry. *Fuel* 190, 359–369.
- Zheng, S.J., Yao, Y.B., Liu, D.M., Cai, Y.D., Liu, Y., 2019b. Nuclear magnetic resonance surface relaxivity of coals. *Int. J. Coal Geol.* 205, 1–13.
- Zheng, S.J., Yao, Y.B., Liu, D.M., Cai, Y.D., Liu, Y., Li, X.W., 2019a. Nuclear magnetic resonance T<sub>2</sub> cutoffs of coals: a novel method by multifractal analysis theory. *Fuel* 241, 715–724.